# Dynamics of a Lennard-Jones system close to the glass transition

U. Bengtzelius
*Institute of Theoretical Physics, Chalmers University of Technology, S-412 96 Göteborg, Sweden*
(Received 29 July 1986)

Numerical results on the dynamics in a Lennard-Jones system close to the glass transition are presented, using a kinetic model presented in an earlier paper. The theory is based on the Zwanzig-Mori procedure for deriving formally exact transport equations combined with mode-coupling approximations. Results for a number of different dynamical quantities of experimental interest are presented and the model is shown to reproduce many of the characteristic features of a liquid-glass transition. Comparisons are made with available computer simulation data and analytical results for the same mode-coupling model.

## I. INTRODUCTION

Experiments on a variety of glass-forming systems have revealed some quite remarkable behavior when approaching the glass transition point. Volume, entropy, and free energy change continuously when passing through the transition, whereas the compressibility, the thermal expansion coefficient, and the specific heat seem to change discontinuously. There is always some smearing of the transition due to the fact that the cooling rate has to be compatible with laboratory and glass-forming conditions. The viscosity increases many orders of magnitude when approaching the transition point from the supercooled liquid side and the temperature dependence shows a characteristic non-Arrhenius behavior. This implies that the diffusion process is not of a simple activated type. Extremely slow structural relaxations are observed both when approaching the transition from the liquid and glass side and they are of a characteristic nonexponential type. Structural relaxations are occurring on various time scales, ranging from microscopic all the way to macroscopic times, and various kinds of experimental tools have to be used to cover this extremely broad time region.

Computer simulations have revealed that even such simple systems as hard sphere and Lennard-Jones show a transition from a liquid to a glass, provided that the cooling rate is sufficiently fast to prevent crystallization from occurring. A remarkable fact is that various kinds of systems ranging from polymers to computer systems show a rather universal behavior close to the transition point. This is particularly apparent if one scales time and temperatures in an appropriate way.[1] The above facts suggest that the basic mechanism behind the glass transition is essentially the same in all cases and does not depend sensitively on the specific form of the interaction. This is certainly not true for the crystallization rate nor for the absolute values of the relaxation times. Therefore, one should think of times and temperatures in some scaled units. One may also have to exclude such glasses which form a characteristic network, like $SiO_2$.

The theory of dynamics of simple liquids has by now been brought to maturity. The agreement between the theory, based on the Zwanzig-Mori formalism and mode-coupling approximations, and experimental and computer simulation data on a variety of properties, are quite impressive.[2] In a series of recent papers[3–5] this kind of approach was extended to describe dynamics of supercooled liquids and of glass transitions. It was found that the theory incorporates a mechanism for a transition from a diffusive liquid state to a glassy state with vanishing diffusivity. The quantity of prime interest is the time-dependent density correlation function

$$F(\mathbf{k},t)=\frac{1}{N}\langle \delta n(\mathbf{k},t)\delta n(-\mathbf{k},0)\rangle \ , \tag{1.1}$$

which has been investigated extensively through light scattering and neutron scattering experiments and also through computer simulation. Here $\delta n(\mathbf{k},t)$ is the microscopic density fluctuation around its uniform average value. The glass transition is characterized as a transition from an ergodic to a nonergodic behavior and the glass shows up as a time-persistent part in $F(\mathbf{k},t)$. In the works referenced above, the ergodicity breaking originates from a strong nonlinear coupling of the density fluctuations. The theory was later generalized by Bengtzelius and Sjögren[6] to include coupling between density and temperature fluctuations, in this way recovering the complete generalized hydrodynamic expression for the density correlation function with frequency and wave-vector-dependent transport coefficients entering.[7] Although the freezing condition was unaltered by this improvement, it provided some exact relations for the discontinuities in the compressibility, the thermal expansion coefficient, and the specific heat.

It is important to notice that in the theory of Bengtzelius, Götze, and Sjölander[4] (hereafter referred to as I) the ergodicity breaking arises from strong coupling of density fluctuations whose wave vectors are within the main peak of the static structure factor $S(k)$. These reflect the relaxation of the local structure and trigger the transition. It is of importance to stress that the bracket $\langle\ \rangle$ used in Eq. (1.1) and throughout denotes an average over the equilibrium liquid ensemble. In our treatment the liquid is always the true equilibrium state, since crystallization is prevented, and the transition to a nonergodic state comes out from solving the nonlinear equations self-consistently. The frozen structure we obtain here would correspond to the structure one has to introduce *a*

 

*priori* when a restricted-ensemble approach is used. A purely hydrodynamic approach as presented by Das *et al.*,[8] Das and Mazenko,[9] and Siggia[10] differs from our approach on an important point. They consider only the long-wavelength limit whereas in our case the self-consistency requires that we consider all wavelengths and frequencies simultaneously. The hydrodynamics then follows as a byproduct.

In paper I the density correlation (1.1) was expressed in terms of a memory function $M(k,t)$. With a mode-coupling approximation for the latter, taking only pairs of density fluctuations into account, a closed equation for $F(k,t)$ was derived with the only input being the static structure factor. Due to the complexity of this equation, a simplification was made by replacing $S(k)$ with a $\delta$ function positioned at the main peak and ignoring all other structure in $S(k)$. This yielded an equation identical to the one analyzed by Leutheusser.[3] The analysis led to a prediction for the density-fluctuation spectrum and to certain scaling laws. In particular, the viscosity $\eta$ was found to diverge at the transition point as $|\varepsilon|^{-1.765}$, where $\varepsilon \propto (T_g - T)/T_g$ and $T_g$ is the glass transition temperature. The diffusion constant would then vanish as $|\varepsilon|^{1.765}$. Recently the power-law hypothesis for the viscosity was tested for a number of real glass-forming substances[11] and the exponents were found to lie in the range 1.6–2.3.

An extended mode-coupling theory was later analyzed in detail by Götze,[12,13] where the results from the simplified model[3,4] emerged as a special case.

The purpose of the present paper is to present detailed numerical calculations on the dynamics based on our full mode-coupling model in I. Comparisons are made with the predictions by Götze[12,13] and with molecular dynamics data by Ullo and Yip.[14] The system we consider is a Lennard-Jones system.

The paper is organized as follows. In Sec. II we present the basic equations used in the numerical analysis, and in Sec. III we summarize the main predictions by Götze.[12,13] Numerical results of our calculations and comparisons with Götze's predictions and with molecular-dynamics data are presented in Sec. IV. In Sec. V we present the main conclusions.

## II. BASIC FORMULAS

The treatment of the density correlation function $F(k,t)$ and the corresponding self part $F^s(k,t)$ follows very closely that of Sjögren,[15] Sjögren and Sjölander,[16] and Wahnström and Sjögren.[17] We shall consider a monatomic system with the atomic mass $m$.

One can always write the correlation function in a generalized hydrodynamic form (see, for instance, Ref. 6)

$$F(k,z) = -S(k)\frac{z + M(k,z)}{z^2 - k^2/m\beta S(k) + zM(k,z)} , \tag{2.1}$$

where $\beta = 1/k_B T$ is the inverse temperature, $S(k)$ is the liquid static structure factor, and $M(k,z)$ is a generalized friction term. $F(k,z)$ is defined as the Laplace transform

$$F(k,z) = i\int_0^\infty dt\, e^{izt} F(k,t), \quad \mathrm{Im}z > 0 \tag{2.2}$$

and similarly for $M(k,z)$ and other dynamical quantities. The expression for $F^s(k,t)$ is the same as (2.1), except that $S(k)$ is replaced by unity and another memory function $M^s(k,z)$ enters. The corresponding spectral function is the cosine transform of $F(k,t)$, i.e.,

$$F''(k,\omega) = \mathrm{Im}F(k, z = \omega + i0^+) . \tag{2.3}$$

For convenience we rewrite Eq. (2.1) in the form[4]

$$\frac{R(k,z)}{1 + zR(k,z)} = \frac{m\beta S(k)}{k^2}[z + M(k,z)] , \tag{2.4}$$

with $R(k,z) = F(k,z)/S(k)$, and similarly for $F^s(k,z)$.

Both $M(k,t)$ and $M^s(k,t)$ include effects from single binary collisions as well as more collective events which give rise to a decay on a much slower time scale. Considering glass transitions we need only worry about the slowly decaying part. However, if we want to compare our results with computer-simulation data we may have to include the short-time part as well, which is definitely necessary in the ordinary-liquid region. The collective events seem to be quite well represented through a low-order mode-coupling approximation.[15] For $F^s(k,t)$ the single binary collisions are well taken care of through a slight generalization of the ordinary Fokker-Planck equation, introduced originally by Lebowitz, Percus, and Sykes[18] and Akcazu, Corngold, and Duderstadt.[19] Following Sjögren[15] and Wahnström and Sjögren[17] we split $F^s(k,t)$ into a binary-collision part $F^{sB}(k,t)$, being the solution of our generalized Fokker-Planck equation, and a more collective part. Using their results and their notations we obtain after some rewriting

$$\frac{R(k,z)}{1 + zR(k,z)} = S(k)\left[\frac{F^{sB}(k,z)}{1 + zF^{sB}(k,z)} + \frac{m\beta}{k^2}[\Gamma_{11}^B(k,z) - \Gamma_{11}^{sB}(k,z)]\right] + \frac{m\beta S(k)}{k^2} R_{00}^l(k,z) \tag{2.5}$$

and

$$\frac{F^s(k,z)}{1 + zF^s(k,z)} = \frac{F^{sB}(k,z)}{1 + zF^{sB}(k,z)} + \frac{m\beta}{k^2} R_{00}^s(k,z) . \tag{2.6}$$

Here $\Gamma_{11}^B(k,t)$ and $\Gamma_{11}^{sB}(k,t)$ extend essentially over the time for a binary collision and the latter one enters in the equation for $F^{sB}(k,z)$. Following Ref. 15 we make a Gaussian ansatz for their time dependence and determine the corresponding relaxation times from the short-time expansion of $R(k,t)$ and $F^s(k,t)$ up to power $t^6$. When considering small frequencies we can take the zero-frequency limit of all the binary parts in (2.5)–(2.6) and we are then back to the full model in I. The essential dynamics are then connected with collective events entering in $R_{00}^l$ and $R_{00}^s$. For these we make the lowest-order mode-coupling approximation[15]

$$R^{l}_{00}(k,t)=\frac{n}{2m\beta}\int\frac{d\mathbf{k}'}{(2\pi)^3}\{(\hat{\mathbf{k}}\cdot\mathbf{k}')c(k')+[\hat{\mathbf{k}}\cdot(\mathbf{k}-\mathbf{k}')]c(|\mathbf{k}-\mathbf{k}'|)\}^2$$
$$\times S(k')S(|\mathbf{k}-\mathbf{k}'|)[R(k',t)R(|\mathbf{k}-\mathbf{k}'|,t)-R^{B}(k',t)R^{B}(|\mathbf{k}-\mathbf{k}'|,t)] \quad (2.7)$$

and

$$R^{s}_{00}(k,t)=\frac{n}{m\beta}\int\frac{d\mathbf{k}'}{(2\pi)^3}[(\hat{\mathbf{k}}\cdot\mathbf{k}')c(k')]^2S(k',t)R(k',t)[F^{s}(|\mathbf{k}-\mathbf{k}'|,t)-F^{0}(|\mathbf{k}-\mathbf{k}'|,t)] . \quad (2.8)$$

Here, the interaction potential enters only through the direct correlation function $c(k)=[S(k)-1]/nS(k)$. Furthermore, $F^{0}(k,t)=\exp[-k^2t^2/2m\beta]$ is the free-particle value of $F^{s}(k,t)$ and $R^{B}(k,t)$ is approximated by

$$R^{B}(k,t)=[F^{0}(k,t)/F^{s}(k,t)]R(k,t) . \quad (2.9)$$

The subtractions in (2.7) and (2.8) are necessary in order to compensate for the fact that single binary events are included elsewhere. This implies that the mode-coupling terms start as $t^4$. It takes a certain time to build up these collective effects, but once there they will persist for quite some time. The procedure is such that the frequency moments of $R(k,t)$ and $F^{s}(k,t)$ are by definition exact up to sixth order. However, in the present calculation the binary collision time for $\Gamma^{B}_{11}$ is approximated by that for $\Gamma^{sB}_{11}$.[15] One should be aware of the fact that the short-time events are included in a realistic way but that the quantitative accuracy is not very high.

In comparing with Ref. 15 we notice that here we have ignored all mode-coupling terms involving currents. These would play no essential role for our discussion of the glass transition, except possibly renormalizing the transition temperature slightly. The approximations in (2.7) and (2.8) also imply a neglect of the coupling between density and temperature fluctuations, and for a generalization thereof we refer to an earlier paper.[6] Again, this is not essential for our present discussion.

Equations (2.5) and (2.6) are now two coupled closed equations which we have solved through an iteration procedure. Once the numerical solution was obtained, the self-diffusion constant, the velocity correlation function, and the mean-square displacement were calculated from[16]

$$D=i/[m\beta\Gamma^{s}_{11}(k=0,z=0)] , \quad (2.10)$$

$$\psi(z)\equiv(3k_BT/m)i\int_0^\infty dt\, e^{izt}\langle\mathbf{v}(t)\cdot\mathbf{v}(0)\rangle$$
$$=-1/[z+\Gamma^{s}_{11}(k=0,z)] , \quad (2.11)$$

$$\langle\Delta r^2(t)\rangle=2\int_0^t d\tau(t-\tau)\langle\mathbf{v}(\tau)\cdot\mathbf{v}(0)\rangle . \quad (2.12)$$

The glass transition is characterized by the point where

$$f(k)\equiv R(k,t=\infty) \quad (2.13)$$

changes from zero to a finite value. Similarly we define

$$f^{s}(k)\equiv F^{s}(k,t=\infty) , \quad (2.14)$$

and the two form factors give the intensity of the strictly elastic parts in coherent and incoherent scattering of neutrons, respectively.

## III. THE PREDICTIONS OF GÖTZE

In two recent papers[12,13] Götze has analyzed Eq. (2.4), considering a more general functional relation between $M(k,t)$ and $R(k,t)$ than assumed here. Therefore, his conclusions should have a rather general validity.

Introducing a parameter $\varepsilon$ to characterize the distance from the glass transition point—it can be $\varepsilon\propto(T_g-T)/T_g$ or $\varepsilon\propto(n-n_g)/n_g$ depending on whether temperature or density is changed—he showed that the form factor $f(k)$ varies as

$$f(k)=\begin{cases} f^{c}(k)+a\varepsilon^{1/2}h^{c}(k), & \varepsilon\to0^+ \\ 0, & \varepsilon<0 , \end{cases} \quad (3.1)$$

where

$$h^{c}(k)=[1-f^{c}(k)]^2l^{c}(k) \quad (3.2)$$

and $a$ is a specified number.[12,13] Here $f^{c}(k)$ is the limit value obtained for $f(k)$ when approaching the transition point from the glass side and $l^{c}(k)$ is the right-hand eigenvector of a certain stability matrix. Only the largest eigenvalue of this matrix and the corresponding eigenvectors are of interest and the glass transition occurs when this eigenvalue, being less than one in the glass region, reaches unity.

When restricting ourselves to the form of $M(k,t)$ used in this paper, the stability matrix is obtained from $R^{l}_{00}$ in Eq. (2.7). Replacing $R(k,t)$ by $f(k)$ and writing $[m\beta S(k)/k^2]R^{l}_{00}=\hat{\mathbf{F}}_k(f_q)$ in the matrix form

$$\hat{\mathbf{F}}_k(f_q)=\tfrac{1}{2}\sum_{q,p}V(k;q,p)f_pf_q , \quad (3.3)$$

the stability matrix is defined as

$$C_{kq}=\frac{\delta\hat{\mathbf{F}}_k}{\delta f_q}(1-f_q)^2=\sum_p V(k;q,p)f_p(1-f_q)^2 . \quad (3.4)$$

Its largest eigenvalue and the corresponding right-hand and left-hand eigenvectors, denoted by $l_k$ and $\hat{l}_k$, have been determined numerically after discretizing the wave-vector space and introducing a fine mesh. Following Götze, we normalize the eigenvectors according to

$$\sum_k\hat{l}_kl_k=1, \quad \sum_k\hat{l}_kl_k^2(1-f_k)=1 . \quad (3.5)$$

The various scaling-law exponents are uniquely determined by one single parameter

$$\lambda=\sum_{k,q,p}\hat{l}_k C_{k,q,p} l_q l_p \ , \tag{3.6}$$

where

$$C_{k,q,p}=\frac{1}{2}\frac{\delta\hat{\mathbf{F}}_k}{\delta f_q\,\delta f_p}(1-f_q)^2(1-f_p)^2$$

$$=\tfrac{1}{2}V(k;q,p)(1-f_q)^2(1-f_p)^2 \ . \tag{3.7}$$

The density-fluctuation spectrum is ruled by two scaling frequencies

$$\omega_c \propto |\varepsilon|^a, \quad \omega_c' \propto |\varepsilon|^\gamma \ , \tag{3.8}$$

where $a=1/(1-x)$ and $\gamma=[1/(1-x)]+[1/(y-1)]$. The values of $x$ and $y$ are obtained as the two solutions for $\xi$ of the equation

$$\lambda=\Gamma^2\left[\frac{1+\xi}{2}\right]\Big/\Gamma(\xi) \ , \tag{3.9}$$

where $\Gamma(\xi)$ being the $\gamma$ function. A third frequency $\omega_0$, being of the order of the Debye frequency, characterizes the time scale of the true microscopic motion.

In the glass and close to the transition point we have

$$R(k,t)=f(k)+A_+\varepsilon^{1/2}h(k)f_+(\omega_c t) \tag{3.10}$$

for times large compared to $1/\omega_0$. On the liquid side we have

$$R(k,t)=f^c(k)+A_-|\varepsilon|^{1/2}h^c(k)f_-(\omega_c t) \tag{3.11}$$

for $1/\omega_0 \ll t \ll 1/\omega_c'$. The two $A_+$ and $A_0$ are unspecified but interrelated constants and $f_\pm(\tau)$ are two scaling functions, which, Laplace transformed, satisfy the equations

$$-f_+(\zeta)+\frac{1}{\lambda}\zeta f_+^2(\zeta)+i\int_0^\infty d\tau e^{i\zeta\tau}f_+^2(\tau)=0 \tag{3.12}$$

and

$$\frac{1}{\zeta}+\frac{1}{\lambda^c}\zeta f_-^2(\zeta)+i\int_0^\infty d\tau e^{i\zeta\tau}f_-^2(\tau)=0 \tag{3.13}$$

with $\zeta=z/\omega_c$ and $\tau=\omega_c t$.

In particular, one finds for the corresponding spectral functions

$$\begin{aligned} &R_+''(k,\omega)\propto(\omega_c/\omega)^{(1+x)/2}, \quad \omega_c\ll\omega\ll\omega_0 \ , \\ &R_-''(k,\omega)\propto(\omega_c/\omega)^{(1+x)/2}, \quad \omega_c\ll\omega\ll\omega_0 \ , \end{aligned} \tag{3.14}$$

and

$$R_-''(k,\omega)\propto(\omega_c/\omega)^{(1+y)/2}, \quad \omega_c'\ll\omega\ll\omega_c \ . \tag{3.15}$$

Apart from this, $R_+''(k,\omega)$ contains a strictly elastic component with the strength $f(k)$. For $R_-''(k,\omega)$ it still remains to determine the frequency dependence for $\omega<\omega_c'$.

The simplified model in paper I yields the value $\lambda=\frac{1}{2}$ and this leads to $x=0.209$ and $y=3.0$. $f_-(\omega_c t)$ was found to decay exponentially for $t>1/\omega_c'$ and the diffusion constant is proportional to $\omega_c'$ leading to the exponent $\gamma=1.76$. For the full model in I no exact results are known in this asymptotically small-frequency region.

## IV. PRESENTATION OF NUMERICAL RESULTS

We have considered a one-component system with the atoms interacting via the Lennard-Jones potential

$$v(r)=4\varepsilon[(\sigma/r)^{12}-(\sigma/r)^6] \ . \tag{4.1}$$

In the presentation of the data we shall use reduced units, where $\varepsilon$, $\sigma$, and $m$ are the units for energy, length, and mass, respectively. For argon the usual choice is $\varepsilon/k_B=120$ K and $\sigma=3.4$ Å. The corresponding unit of time is then $\tau_0=(m\sigma^2/\varepsilon)^{1/2}=2.15\times10^{-12}$ s and that of the diffusion constant $D_0=5.37\times10^{-4}$ cm$^2$/s. All quantities in reduced units are marked by an asterisk, e.g., $T^*=k_BT/\varepsilon$ for the reduced temperature. The calculations were carried out for $T^*=0.6$ and $\varepsilon=(n-n_g)/n_g$ close to zero, with $n_g$ being the glass transition density.

The static structure factor, which enters as an input in Eqs. (2.5) and (2.6) was calculated separately using the optimized random-phase approximation.[20] This was presented already in an earlier paper[21] where results were given for the glass transition points of some different systems.

In the three-dimensional mode-coupling integrals (2.7) and (2.8) one angular integration is trivial and with a suitable variable substitution we end up with two-dimensional integrals in $\mathbf{k}$ space (see paper I). These were calculated employing the Simpson integration procedure. By using a special technique of storing intermediate results from the inner integration the computational time increases linearly with the number of $k$ values rather then quadratically. The resulting equations for $R(k,z)$ and $F^s(k,z)$ were iterated until convergence was achieved. For the binary collision parts we followed the numerical procedure of Sjögren[15] and Wahnström and Sjögren.[17]

The integrations were done up to value $k^*=30$ and with a mesh of $\Delta k^*=0.15$ In each iteration the mode-coupling terms $R_{00}^l$ and $R_{00}^s$ in Eqs. (2.7) and (2.8) were calculated in time and then Laplace transformed and added to the binary parts in order to get the next iterated values for $R(k,z)$ and $F^s(k,z)$. The time integrations had to be carried out with particular care since a very large time interval was covered. For that reason the total interval was first split up into several subintervals of increasing length for increasing times. Each of the subintervals was then given a fixed grid. Correspondingly, the frequency interval was first split into subintervals of decreasing length with decreasing frequencies and each was given a fixed grid. In this way we could handle simultaneously narrow quasielastic peaks and broad inelastic bands in the frequency spectrum. It turned out to be important to check that the total time interval chosen at the beginning was large enough. Therefore, after the first iteration procedure had converged we extended the total time span by adding one subinterval, implying a splitting of the smallest frequency subinterval into two, and then continued the iteration until new convergence was achieved. If necessary, this was continued until no noticeable change was found in the final results. By transforming from frequen-

cy to time and then back to frequency again we could check the accuracy of our procedure. When carrying out an iteration for a new density closer to the transition point we used the previous calculated $R(k,z)$ and $F^s(k,z)$ as the starting point for the iteration. We tested that the same results for $R(k,z)$ and $F^s(k,z)$ were achieved irrespective of whether the starting values were taken from a higher or lower density. For the density closest to the transition point in the liquid, 120 iterations were required, which took 30 h of computer time on our Gould 32/8780.

The calculations were carried out for liquid and glass densities for $T^*=0.6$. In the glass the asymptotic values for $R^l_{00}(k,t)$ and $R^s_{00}(k,t)$ were subtracted in each iteration before carrying out the Laplace transformations. The form factors obtained in this way could then be checked against those calculated directly as in Ref. 21.

In addition to the calculations above we have determined the eigenvalues and eigenvectors of the corresponding Götze stability matrix (3.4). The form factors were calculated as in Ref. 21 and the transition point was found from this to lie in the range $0.9601 < n_g^* < 0.9602$. The main results are as follows.

(i) For $n^*=0.9602$ the largest eigenvalue was found to be 0.993, whereas the next largest is 0.283 with a negligible imaginary part. Changing to a slightly higher density, $n^*=0.9603$, the largest eigenvalue is 0.986 and it decreases to 0.912 for $n^*=0.9654$. This implies that the glass transition occurs at a slightly lower value than $n^*=0.9602$. The largest eigenvalue follows very closely a $\varepsilon^{1/2}$ dependence as predicted by Götze.[12,13]

(ii) The scaling parameter $\lambda$ in Eq. (3.6) was calculated to $\lambda=0.714$, which through Eq. (3.9) gives $x=0.358$ and $y=2.234$ for $n^*=0.9602$ and $T^*=0.6$.

Our main results will be presented through a series of figures, to which we make appropriate comments. In Fig. 1 we show the calculated static structure factor and the form factors $f(k)$ and $f^s(k)$ at the critical density $n_g^*=0.9602$. The right-hand eigenvector $l(k)$, corresponding to the largest eigenvalue of the stability matrix, is shown in the insert. We find that the form factors approach their critical values as $\varepsilon^{1/2}$ in agreement with the prediction of Götze, Eq. (3.1). The form factors are very similar to those in paper I for a hard-sphere system, except in the range $1 < k^* < 5$. This difference is due to the bump in $S(k)$ in the same $k$ region and could be an artifact of the optimized random-phase approximation. Fortunately, this $k$ region has a very small influence on our main results and has a negligible effect on the value of our critical density.

Ullo and Yip[14] have carried out molecular-dynamics simulations for a truncated and shifted Lennard-Jones potential. For the same potential we reported a critical density of $n_g^*=0.965$ for $T^*=0.6$ in Ref. 21. The values of $f(k)$ produced by the simulations ranged from roughly 0.5 for small $k$ values to 0.8 around the main peak in $S(k)$ ($k^*\approx 7$), which is in reasonable agreement with our findings. From their data on pressure versus density at $T^*=0.6$ they estimated an $n_g^*\approx 1.02$, whereas their diffusion constant seems to vanish near $n^*\approx 1.1$. Hence, in our predictions the transition occurs at a lower density than in Ref. 14. In Ref. 21 the possible sources of errors

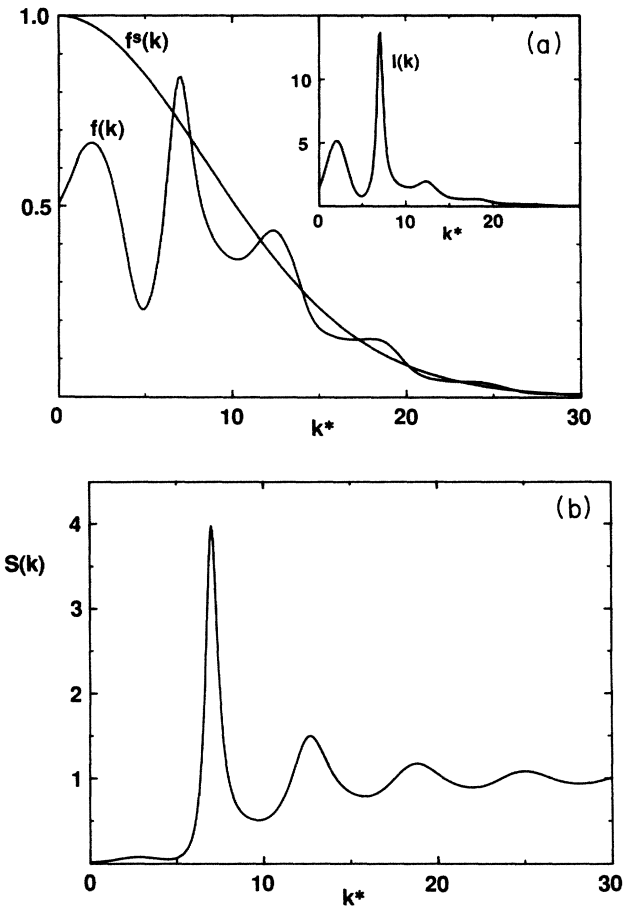


FIG. 1. (a) Form factors $f^c(k)$ and $f^{sc}(k)$ at the glass transition point $n_g^*=0.9602$, $T^*=0.6$. The inset shows the right-hand eigenvector $l^c(k)$ of the Götze stability matrix. Reduced units are used here and henceforth. (b) $S(k)$ of the Lennard-Jones system at the glass transition point, calculated within the optimized random-phase approximation. Main peak position is at $k^*=7.0$.

entering through our approximations were discussed. However, the main interest concerns the dynamics close to the transition and that is not affected by the absolute position of this point.

Figure 2 shows the decay of $R(k,t)$ in the liquid region at $k^*=7$. The various densities are expressed by the separation parameter $\varepsilon$. For comparison we also include results corresponding to the triple point of argon. The maximum time probed by Ullo and Yip[14] is $48\tau_0$ ($\approx 10^{-10}$ s) while our calculations extend out to $0.4\times 10^6\tau_0$ ($\approx 10^{-6}$ s) for the states closest to $n_g^*$. In order to compare our results with those obtained by Ullo and Yip (Fig. 3 in Ref. 14) we have to relate their densities to the separation parameter $\varepsilon$. For instance, the value $\varepsilon=-0.052$ would correspond to $n^*=1.04$, if their $n_g^*$ is assumed to be 1.10 and we want to be at the same distance from the transition point. Even though there is a qualitative agreement between our results and those of Ullo and Yip, their time interval seems too short for having a detailed test of the theory. One should notice that all the curves in Fig. 2 refer to the supercooled liquid state. As we will see, only

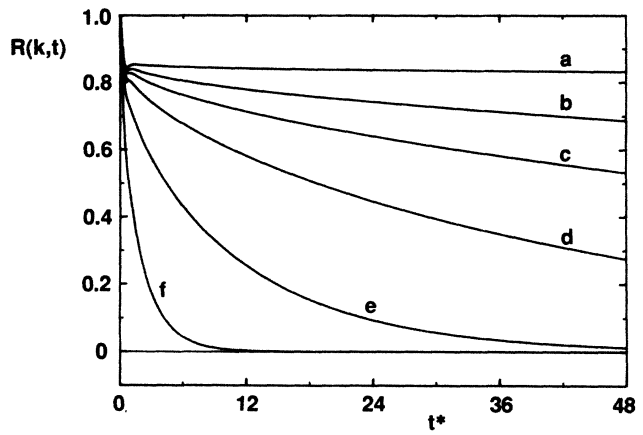


FIG. 2. Normalized density correlation function $R(k,t)$ vs $t^*$ at $k^*=7.0$ and for curve $A$, $\varepsilon=-0.000\,31$ (1.099); curve $B$, $\varepsilon=-0.0054$ (1.094); curve $C$, $\varepsilon=-0.0106$ (1.088); curve $D$, $\varepsilon=-0.021$ (1.072); curve $E$, $\varepsilon=-0.052$ (1.043). Curve $F$ corresponds to the triple point $n^*=0.844$, $T^*=0.722$ for argon. The numbers in parentheses give the corresponding reduced densities in Fig. 3 of Ref. 14, assuming their $n_g^*=1.10$. Negative values for $\varepsilon$ refer to the liquid state.

the top curve is sufficiently close to the transition point to reveal the interesting asymptotic behavior.

In order to show $R(k,t)$ over a longer time interval we present in Fig. 3 our data on a logarithmic time scale. The solid curves are for $k^*=7.0$ and various $\varepsilon$, whereas the dashed curve refers to $k^*=6.0$ and $\varepsilon=-0.000\,31$, and the two straight lines show the values of the form factor at the critical density for the two $k$-values considered. The longest time considered here corresponds for argon to $10^{-6}$ s. Being close to the transition point we clearly see three separate time regions where the first one is truly microscopic and extends to times of order $\tau_0$. It is obvious

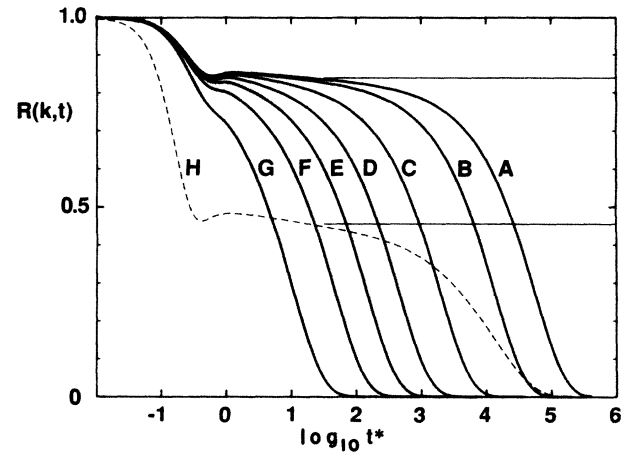


FIG. 3. $R(k,t)$ vs $\log_{10}t^*$ at $k^*=7.0$ (solid curves) and $k^*=6.0$ (dashed curve) and curve $A$, $\varepsilon=-0.000\,31$; curve $B$, $\varepsilon=-0.000\,73$; curve $C$, $\varepsilon=-0.0023$; curve $D$, $\varepsilon=-0.0054$, curve $E$, $\varepsilon=-0.0106$; curve $F$, $\varepsilon=-0.021$; curve $G$, $\varepsilon=-0.052$; curve $H$, $\varepsilon=-0.000\,31$. The straight lines show the values of the form factor at the critical density for $k^*=7.0$ and 6.0.

that the initial decrease of $R(k,t)$ is caused by atomic vibrations analogous to those in crystals. This part is essentially unchanged when moving into the glass. After a microscopic time $R(k,t)$ stays approximately constant for a long time with no noticeable diffusion process occurring and this part is essentially the same as in the glass. In the third region $R(k,t)$ decreases slowly to zero due to diffusion, whereas $R(k,t)$ would stay constant in the glass. The different time evolutions give rise in the spectral function to two overlapping quasielastic peaks with different widths and a broad inelastic part extending to the order Debye frequency. For the curves corresponding to $\varepsilon=-0.0054$ in Fig. 2 and Fig. 3, the intermediate time region cannot really be separated out. The quasielastic peak in the spectral function would simply be interpreted as due to ordinary diffusion processes.

In Fig. 4 we show the $k$ dependence of $R(k,t)$ at four different times, $t^*=10^2$, $10^3$, $10^4$, and $10^5$, and $\varepsilon=-0.000\,31$. We notice that for the shortest time, $t^*=10^2$, $R(k,t)$ has essentially the same structure as $f(k)$ in Fig. 1. This tells us that on this time scale the liquid appears frozen. Another point to notice is that the time decay of $R(k,t)$ for $k$ values at the main peak in $S(k)$ ($k^*\approx 7$) is considerably slower than for other $k$ values. As time increases it seems as if the region of $k$ values of significance narrows around $k^*=7$. This would become more obvious if we normalize the curves to have the same maximum value. One may speculate that for very long times the dynamics is well described by the simplified model in paper I where only one wave number entered in the memory function.

We have made an interesting observation concerning the $k$ dependence of $R(k,t)$, which is demonstrated in Fig. 5 for two different times, $t^*=10^3$ and $t^*=10^5$, and $\varepsilon=-0.000\,31$. For the shorter time $R(k,t)$ is very well described by (for notations see Sec. III)

$$R_1(k,t)=f^c(k)\exp[-a(t)h^c(k)/f^c(k)]\,, \tag{4.2}$$

while for the longer time we have excellent agreement with

$$R_2(k,t)=b(t)\exp[-c(t)h^c(k)/f^c(k)]\,, \tag{4.3}$$

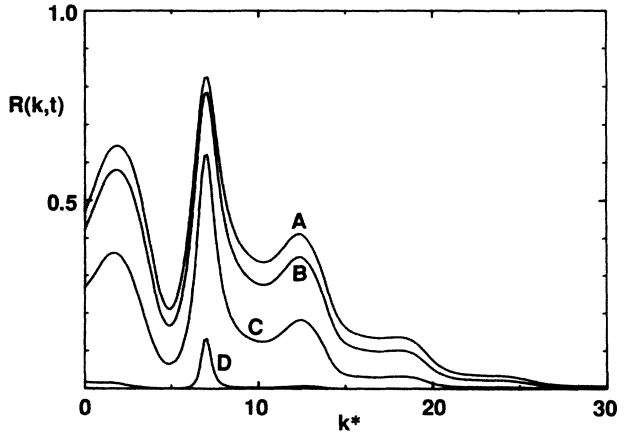


FIG. 4. $R(k,t)$ vs $k^*$ for $\varepsilon=-0.000\,31$ and curve $A$, $t^*=10^2$; curve $B$, $t^*=10^3$; curve $C$, $t^*=10^4$; curve $D$, $t^*=10^5$.

where $a(t)$, $c(t)$, and $b(t)$ are $k$ independent. Here $a(t)$ was adjusted to give agreement with our calculated $R(k,t)$ at $k^*=7.0$ and in (4.3) $b(t)$ and $c(t)$ were adjusted to give agreement at $k^*=7.0$ and 24.0. The first ansatz (4.2) is consistent with the general results of Götze for $1/\omega_0 \ll t \ll 1/\omega_c'$ and we obtain Eq. (3.11) by expanding the exponential term in (4.2) to linear order in $a(t)$ and identifying $a(t)$ with $A_- |\varepsilon|^{1/2} f_-(\omega_c t)$. The same ansatz is found to hold equally well for $t^*=10^2$ and is also reasonable for $t^*=10^4$. However, when diffusion processes become dominant there are large deviations, as shown in Fig. 5(b), and Eq. (4.3) applies better. The exponential form seems still to hold but the prefactor becomes time dependent. Since $[h^c(k)/f^c(k)]$ has its minimum at $k^*=7.0$, $R(k,t)$ decays most slowly for that wave number and this is consistent with what was found in Fig. 4.

The quantity one normally measures is the spectral function. Both in order to cover a very wide range of peak values and frequencies and to extract scaling-law exponents most easily we plot in Fig. 6 $\log_{10}R''(k,\omega)^*$ versus $\log_{10}\omega^*$ for $k^*=7.0$. A purely Lorentzian form for $R''(k,\omega)^*$ gives for large $\omega^*$ a straight line with the slope $-2$. As for the simplified model in paper I we find, when approaching the transition point from the liquid

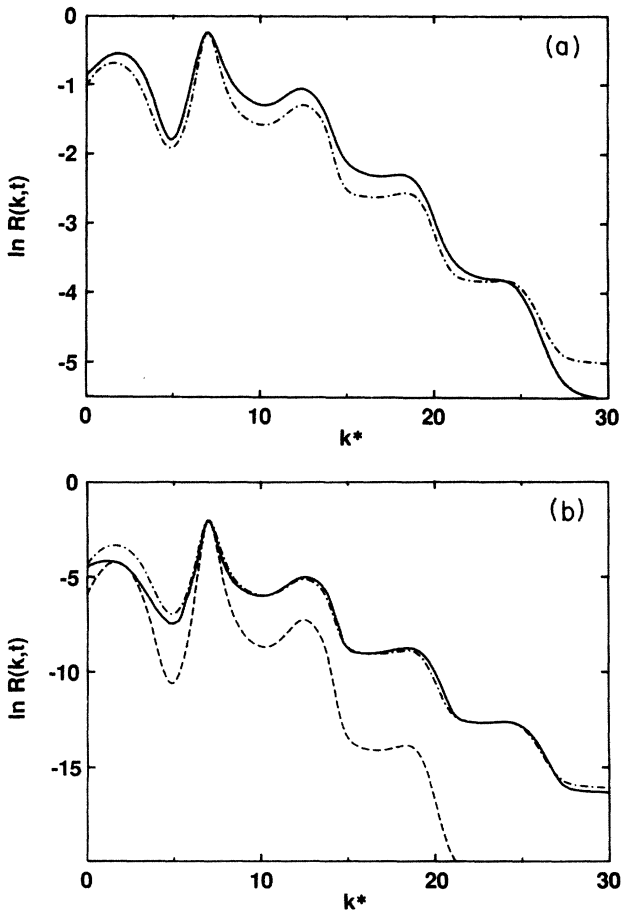


FIG. 5. (a) $\ln[R(k,t)]$ vs $k^*$ for $t^*=10^3$ (solid curve). The dashed curve represents a fit to Eq. (4.2) [completely overlapping $\ln R(k,t)$] and the dot-dashed curve a fit to Eq. (4.3). (b) Corresponding comparison for $t^*=10^5$.

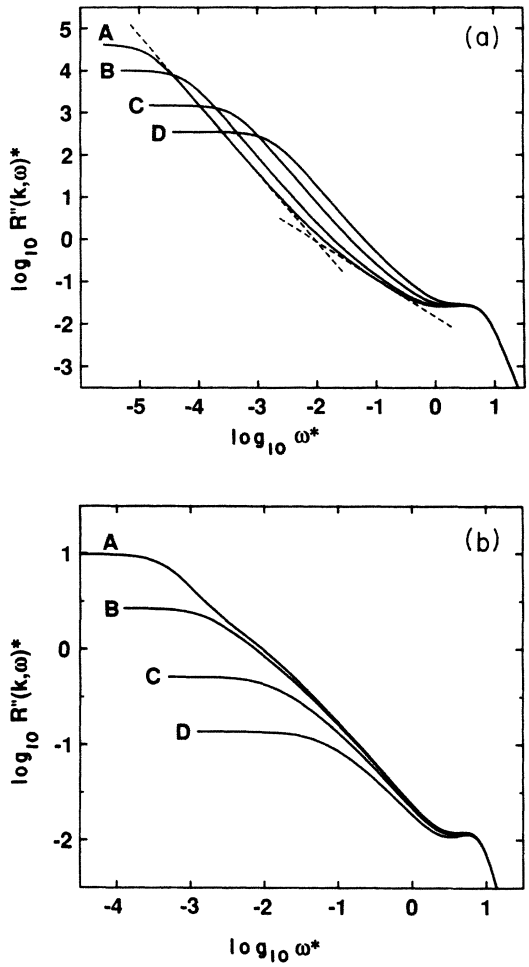


FIG. 6. (a) $\log_{10}[R''(k,\omega)]$ in reduced units vs $\log_{10}\omega^*$ at $k^*=7.0$ for curve $A$, $\varepsilon=-0.00031$; curve $B$, $\varepsilon=-0.00073$, curve $C$, $\varepsilon=-0.0023$; curve $D$, $\varepsilon=-0.0054$. The dashed lines indicate the approximately linear regions from where the slopes $-1.63$ and $-0.9$ are extracted. (b) Corresponding curves on the glass side for the same distances from the glass transition point.

side, a tendency of a quasielastic double-peak structure [Fig. 6(a)]. From curve $A$ we can for $-4.5<\log_{10}\omega^*<-3$ extract a straight line with the slope $-1.63$ and this is not consistent with an exponential decay in time. We notice that the other curves for larger $|\varepsilon|$ values give essentially the same value for the slope. For the simplified model the numerical solution gave a slope $-1.9$, where the exact value is $-2$. The discrepancy shows that one has to be very close to the transition point before the proper asymptotic value is reached.

The other component of the double-peak structure can be seen from the approximately straight line for $-1.5<\log_{10}\omega^*<-0.5$ with the slope $-0.9$. The corresponding value for the simplified model is $-0.605$. Notice that the two peaks are much better separated in the simplified model. One should keep in mind that the separation parameter $\varepsilon$ defined in this paper is not identical with that in paper I. It is obvious that one has to consider extremely small $\varepsilon$ values in order to see clearly the double-peak structure. For $\log_{10}\omega^*>0$ we are in the

microscopic-frequency region, where phononlike excitations dominate.

The corresponding results for the glass are shown in Fig. 6(b). Here the narrower one of the quasielastic peaks on the liquid side has become strictly elastic and is not shown in the figure. For $-1.5<\log_{10}\omega^*<-0.5$ we can extract a straight line with the slope $-0.8$, which is roughly the same as for the liquid.

The peak heights are found to scale as $1/|\varepsilon|^{\alpha}$ with the exponent $\alpha=1.67$ on the liquid side and $\alpha=1.5$ on the glass side.

Another way of presenting some of our data is to plot the half width at half maximum of the spectral function, $\Delta_{1/2}\omega$, versus $\varepsilon$. This is done in Fig. 7 for $k^*=7.0$. For the glass we have subtracted the strictly elastic part. The dashed curves are fits to a power law $\Delta_{1/2}\omega\propto|\varepsilon|^{\gamma}$, where we have extracted a value $\gamma=1.68$ in the liquid and $\gamma=1.8$ in the glass. Since the mode-coupling theories[3-5] also predict a narrowing of the spectrum in the glass, when approaching the transition point, it could be worthwhile to investigate this point experimentally for real glass-forming systems. No conclusion can be drawn from the simulation data of Ullo and Yip[14] (their Fig. 4), since they present results only for one density in the glass. One should also notice that the density region covered in Fig. 7 is very narrow, corresponding to $n^*=1.034$—$1.122$ in Ref. 14. However the corresponding temperature interval, keeping the density fixed, would be larger. From the calculated liquid-glass phase diagram in Ref. 21 we extract $(\Delta T_g^*/\Delta n_g^*)\approx 4.5$ at $T^*=0.6$. The total interval in Fig. 7 would therefore correspond to a temperature interval of $\sim 0.35$ in reduced units. Chen and Huan[22] have recently presented results from photon-correlation measurements for dense microemulsions. Their data (Fig. 2 in Ref. 22) do show a narrowing of the spectrum when the transition point is approached from both sides.

Both dielectric loss experiments[23] and specific-heat spectroscopy[24] can be related to the quantity $\chi''(k,\omega)=\omega R''(k,\omega)$. For a purely exponential decay of $R(k,t)$ the peak in $\chi''(k,\omega)$ is 1.14 decades wide at half maximum. The experiments usually give peaks that are significantly broader than this. In Fig. 8 we show $\chi''(k,\omega)$ versus $\log_{10}\omega^*$ for four different values of $\varepsilon$ and $k^*=7.0$ (solid curves) and for $\varepsilon=-0.000\,31$ and $k^*=6.0$ (dashed curve). For $k^*=7.0$ $\chi''(k,\omega)$ has a width of 1.28 decades and for $k^*=6.0$ this has increased to 1.62 decades, thus being broader than the width corresponding to an exponential decay in time. The peak positions were found to scale as $|\varepsilon|^{\gamma}$ with $\gamma=1.69$, which is consistent with the value of $\Delta_{1/2}\omega$ in the liquid. It is common among experimentalists to fit data to a Kolrausch-Williams-Watts function $R(k,t)\propto\exp[-(t/\tau)^{\beta}]$ where $0<\beta<1$. For such a time dependence we obtain a perfect fit to the curves in Fig. 8 with $\beta=0.88$ for $k^*=7.0$ and $\beta=0.68$ for $k^*=6.0$. Similar results were found by De Raedt and Götze[25] in a somewhat different model.

Concerning a detailed comparison with the predictions of Götze[12,13] for $|\varepsilon|\to 0$, it appears that we have still not come sufficiently close to the transition point. Figure 5(a) shows that the $k$ dependence is very well represented by Eq. (3.11). We find this to be true also in the glass, Eq. (3.10), but due to the fact that $R(k,t)-f(k)$ becomes very small for small $\varepsilon$ and large times the numerical uncertainties are larger. As seen from Fig. (6a) the narrower one of the two quasielastic peaks is well developed and the slope $-1.63$ agrees with the value of Götze, $-(1+y)/2=-1.62$. The other peak is still barely seen and a comparison of $-0.9$ with the asymptotic value for the slope, $-(1+x)/2=-0.68$, may not be meaningful. The peak values in Fig. 6(a) are found to increase as $|\varepsilon|^{-1.67}$, whereas a naive matching to the asymptotic solutions of $R''(k,\omega)$ by Götze gives the value $(\omega_c')^{-1}\propto|\varepsilon|^{-2.37}$. It seems as if the diffusive peak splits off at a higher frequency than assumed in the matching above. Since the numerical accuracy of our data for the glass is more uncertain, we refrain from making any comparisons at this stage. The main reason for showing Fig. 6(b) is to present the qualitative behavior and demonstrate that the half

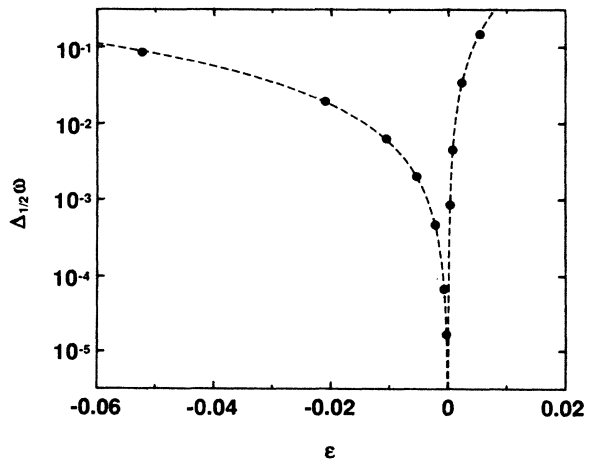


FIG. 7. Half width at half maximum of $R''(k,\omega)$ at $k^*=7.0$ vs $\varepsilon$. The dashed curves represent fits to power laws $|\varepsilon|^{\gamma}$ with $\gamma=1.68$ on liquid side ($\varepsilon<0$) and $\gamma=1.8$ on glass side ($\varepsilon>0$).

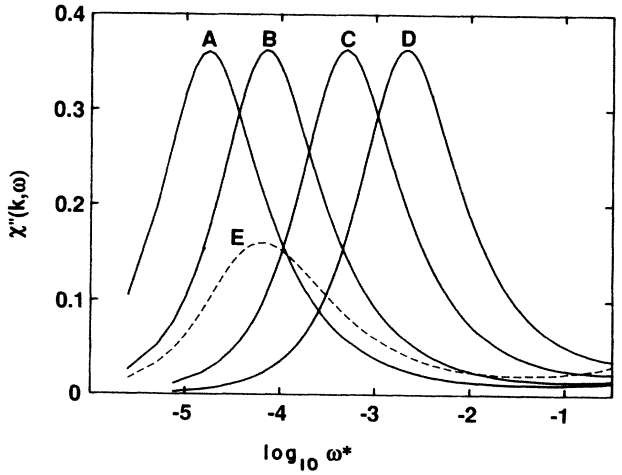


FIG. 8. $\chi''(k,\omega)=\omega R''(k,\omega)$ in reduced units vs $\log_{10}\omega^*$ at $k^*=7.0$ (solid curves) and $k^*=6$ (dashed curve) for curve $A$, $\varepsilon=-0.000\,31$; curve $B$, $\varepsilon=-0.000\,73$; curve $C$, $\varepsilon=-0.0023$; curve $D$, $\varepsilon=-0.0054$; curve $E$, $\varepsilon=-0.000\,31$.

width of the quasielastic peak narrows as the transition is approached.

The experimental data concerning the slow relaxations in the liquid are, as mentioned above, often interpreted in terms of the Kohlraush-Williams-Watts function $\exp[-(t/\tau)^{\beta}]$ with $\beta$ as an adjustable parameter. In Fig. 9 we compare for $k^*=6.0$ our calculated $R(k,t)$ both with a pure exponential and a Kohlrausch-Williams-Watts function, taking the value $\beta=0.68$ from Fig. 8. As seen, we obtain for the latter an excellent agreement over three decades. Similarly, an agreement was found for $k^*=7.0$ with $\beta=0.88$ taken from Fig. 8, and the same analyses carried out for $k^*=0$, this being relevant for comparison with photon-correlation measurements, gives $\beta=0.75$.

If in Eq. (4.2) $a(t)$ is dominated by one term proportional to $t^{\beta}$, all the $k$ dependence in the exponent can be included in $\tau$, and $\beta$ in the Kohlrausch-Williams-Watts function becomes $k$ independent. Since we find a significant $k$ dependence of $\beta$, it implies that $a(t)$ must have a more complicated time dependence over the interval considered. In fact, a closer analysis of our data has shown that somewhat different $\beta$ values have to be chosen depending on the time interval considered. For smaller times we have a smaller $\beta$ and it seems as if $\beta$ approaches unity for asymptotic times. Particularly for $k^*=6.0$ $\beta$ has a plateau value of around 0.7 over two decades in time.

In the remaining figures we present results for the single-particle motion. Figure 10 shows the density dependence of the self-diffusion constant. A logarithmic plot is used and a straight line corresponds to a power law $|\varepsilon|^{\gamma}$. We obtain an exponent $\gamma=1.66$ and this should be compared with the value $\gamma=1.76$ for the simplified model in paper I. In this model the diffusion constant scales with the same exponent as $\omega_c'$, but this is not the case for the present model. The value $\gamma=1.66$ is consistent with the values $\gamma=1.69$ and 1.68 obtained from $\chi''(k,\omega)$ and $\Delta_{1/2}\omega$ in Figs. 7 and 8, whereas for $\omega_c'$ we have $\gamma=2.37$.

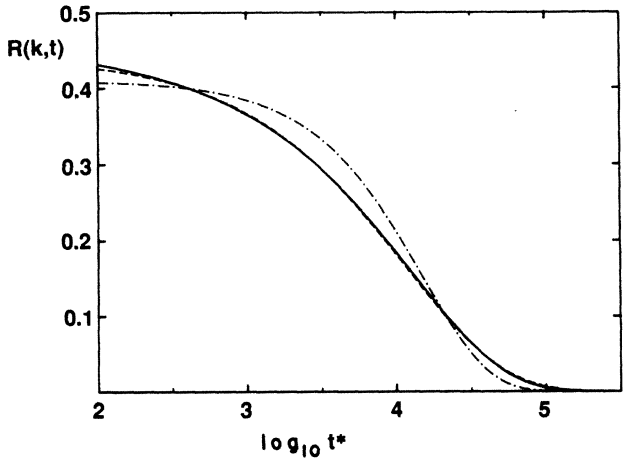


FIG. 9. $R(k,t)$ vs $\log_{10}t^*$ at $k^*=6$ and $\varepsilon=-0.000\,31$ (solid curve). The dashed curve represents a fit to a Kohlrausch-Williams-Watts function with $\beta=0.68$ and the dot-dashed curve a fit to an exponential.

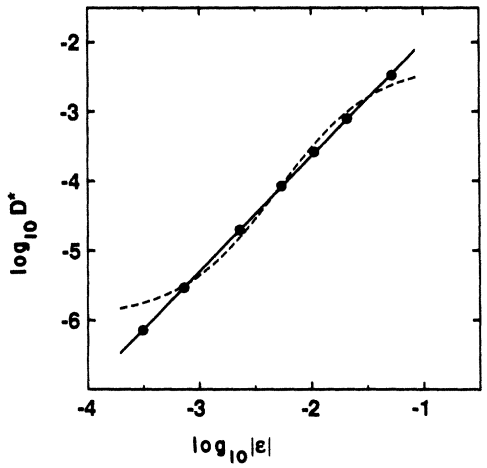


FIG. 10. $\log_{10}D^*$ vs $\log_{10}|\varepsilon|$. The dots are the calculated values and the straight line through them shows a power-law behavior with the exponent $\gamma=1.66$. The dashed curve represents a fit to the Doolittle function (see the text) with $(V_0^{D*})^{-1}=0.965$. The value $\log_{10}D^*=-1.5$ corresponds to the triple point for argon $n^*=0.844$, $T^*=0.722$.

For comparison we also show the kind of fit we obtain using the form $D=A\exp[-B/(V-V_0^D)]$ proposed by Doolittle[26] (dashed curve). It would evidently be difficult to distinguish a power law from a Doolittle behavior in experimental data.

The velocity correlation is shown in Fig. 11 for $\varepsilon=-0.000\,31$. It shows a similar time dependence as found near the triple point, except for the fact that the negative part is deeper and some slow oscillations appear. The rapid initial decrease is mainly due to the binary collisions and should be essentially the same as in the ordinary liquid state. We recall that the area under the curve is proportional to the self-diffusion constant. The corresponding memory function is found to develop an extremely long time tail for small $\varepsilon$ and this is required in order to have a small value for the diffusion constant. Figure 12 presents results for the mean-square displace-

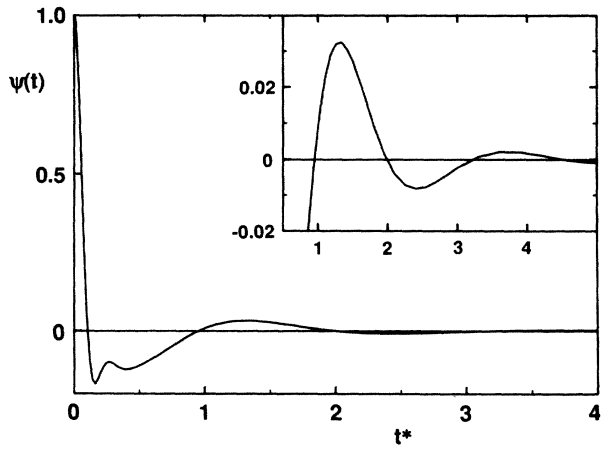


FIG. 11. Normalized velocity correlation function vs $t^*$ for $\varepsilon=-0.000\,31$.

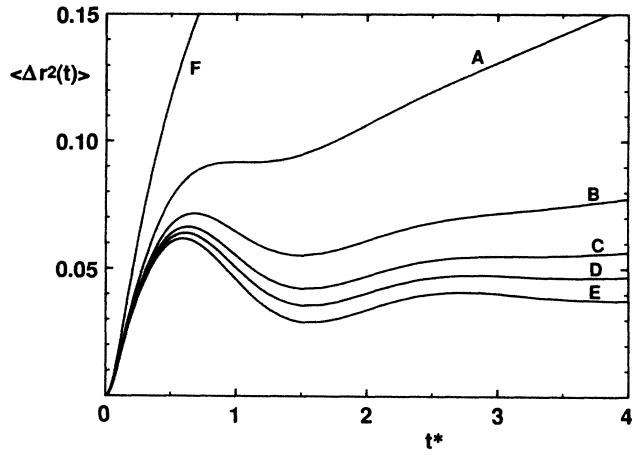


FIG. 12. Mean-square displacements vs $t^*$ for curve $A$, $\varepsilon=-0.052$; curve $B$, $\varepsilon=-0.021$; curve $C$, $\varepsilon=-0.001\,06$; curve $D$, $\varepsilon=-0.000\,54$; curve $E$, $\varepsilon=-0.000\,31$. Curve $F$ is for argon at the triple point $n^*=0.844$, $T^*=0.722$.

ment versus time for different values of $\varepsilon$. For comparison we show also the corresponding curve for the liquid at the triple point. The oscillations observed close to the glass transition point are analogous to the ones obtained in a Debye lattice model.[27]

In Fig. 3 one observes for small $\varepsilon$ a dip in $R(k,t)$ before it reaches an approximately constant value. A similar behavior is found for $F^s(k,t)$ and this point is more clearly illustrated in Fig. 13. Comparing with the two previous figures we can certainly relate the dip to the oscillations in the self-motion. The fact that the dip is larger in $F^s(k,t)$ than in $R(k,t)$ also supports the conclusion that it is more closely connected with the single-particle motion than with collective ones.

## V. CONCLUDING REMARKS

When judging the present model for a liquid-glass transition one must bear in mind that the most simple approximation has been made for the basic part of the memory function. There are ample possibilities of generalizing the model in various directions and one such step was actually done in Ref. 6. The same model with certain improvements, which do not seem essential in the present case, has worked very well quantitatively in the ordinary liquid regime and was found to describe the basic relaxation effects in a proper way.[2] The model presented here does not contain any adjustable parameters and all data were calculated from the given interaction potential, although approximately. The particle-diffusion mechanism is of a nonactivated kind, where an atom has to push the surrounding atoms aside in order to create space for forward motion. The self-consistency implies that the surrounding atoms also have to push their surroundings, and so on. In this way one may argue that the model contains a sequence of diffusion steps. This is analogous to the scenario presented by Palmer *et al.*[28]

We have found that the present model reproduces many of the features characteristic of a system close to the transition point. The main features are as follows.

(i) A strong non-Arrhenius temperature dependence of the viscosity and the diffusivity.

(ii) A strongly nonexponential decay of the slow relaxations in the liquid, following closely a Kohlrausch-Williams-Watts behavior with an exponent significantly small than one.

(iii) Two different slow-relaxation processes, one being arrested at the transition point and the other one remaining on the glass side. This resembles the $\alpha$ and $\beta$ relaxations found experimentally.[29]

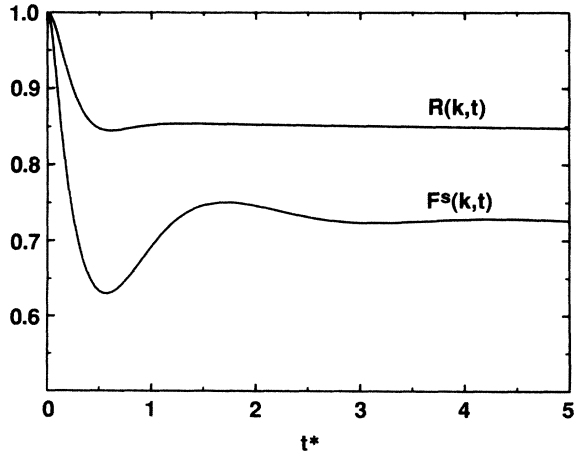


FIG. 13. $R(k,t)$ and $F^s(k,t)$ vs $t^*$ at $k^*=1.0$ and $\varepsilon=-0.000\,31$. Compare with Fig. 3.

Since our present results refer to a Lennard-Jones system any quantitative comparisons should first of all be made with computer simulations. The present theory gives a liquid-glass phase diagram, which is in reasonable quantitative agreement with simulation data.[21] Concerning the basic dynamics, the comparison with data of Ullo and Yip are inconclusive but does not seem to indicate any major shortcomings except for one point which we will come back to later.

The comparison with the predictions from the analysis by Götze[12,13] which gives definite predictions when being asymptotically close to the transition point, are still incomplete. For certain quantities we have excellent agreement while for those referring to the glass our numerical accuracy is not good enough for making definite statements. However, it is evident that the true asymptotic regime is limited to a very narrow region around the transition point. Our numerical results on the liquid side seem to indicate some interesting renormalization in **k** space as time proceeds that may be worthwhile investigating further. The diffusion constant and related quantities are found to scale differently than what is expected from the analysis by Götze. but this could be due to a certain matching assumption of the asymptotic solutions of his scaling equation.

Close to the transition point the theory predicts two different slow-relaxation processes. For a multicomponent system the same qualitative behavior is expected.[13] One

of these exists only in the liquid side and is directly connected with diffusion processes. The only remarkable point here is the nonexponential decay, showing that the diffusion is neither of a simple Brownian type nor of a simple hopping type. This is not that surprising, however, if we consider the state with $\epsilon=-0.000\,31$, where on the average each atom has moved less than one half of the interparticle distance for $\log_{10}gt^*\approx 4.5$. For times of the order $\log_{10}t^*\approx 5.4$ this distance has become larger than the interparticle spacing and here our results indicate that the decay has become essentially exponential.

The other relaxation exists on both sides of the transition and for the liquid it extends only up to times less than the characteristic diffusion time. The liquid appears frozen on this time scale, but in order to see this clearly one has to be extremely close to the transition point so that the diffusion constant is very small.

It is obviously difficult to draw any firm conclusions concerning the multiparticle motions from results for the dynamical structure factor alone. The interpretation of the second slow-relaxation process must therefore be rather speculative. The quantity $S(k)f(k)/f^s(k)$ can be interpreted as a structure factor for the frozen structure with the thermal motion subtracted. This would in a crystal become a set of $\delta(\mathbf{q})$ functions corresponding to the rigid reciprocal lattice giving rise to the strictly elastic Bragg peaks. It is this structure that disappears on melting.

The fluctuations of the frozen structure are in our model described with a dynamical equation that strongly couple wave vectors within the main peak in $S(k)$. The inverse width of this is of the order of ten atomic distances and one might expect the slow motion to be connected with fluctuations in the local ordering over this distance. The observation that the slow motion extends to longer times when approaching the transition point would be due to an incipient structure instability. This is not revealed in the ordinary static structure factor but one may speculate whether higher-order static correlations become singular, perhaps introducing some correlation length which diverges at the transition point.

Even though there are strong qualitative similarities in the behavior of large classes of real glass-forming systems and of the present model, there are also some serious discrepancies. The experiments do not indicate any mathematical singularity at the glass transition point but only some rapid changes. For instance, the viscosity seems to change from a non-Arrhenius temperature dependence to an Arrhenius one and this strongly indicates a change of diffusion mechanism. It seems plausible that such activated processes occur at lower viscosities for simple monatomic systems since the potential barriers may be lower compared to those in complex systems. This would also be consistent with the fact that the barriers for crystallization are much lower. All activated processes are lost because of our mode-coupling approximation for the memory function. An improved version of the theory should therefore include activated processes as well and this would certainly eliminate the above defects. As the present model only applies to one-component systems, an extension to multicomponent systems is urgent. There is no conceptual difficulty in making such an extension but it would lead to considerably more computational work.

## ACKNOWLEDGMENTS

I wish to thank Professor A. Sjölander for his encouragement and support during this work and for valuable comments on the manuscript. I also want to thank Professor W. Götze, Dr. L. Sjögren, and Professor J. Stevens for valuable discussions and comments on this subject, Dr. D. Andersson for helpful comments on the manuscript, and Professor S. Yip for providing additional computer-simulation data. The work is supported by the Swedish Natural Science Research Council.

[1]C. A. Angell and L. M. Torell, J. Chem. Phys. **78**, 937 (1983).
[2]See, e.g., A Sjölander, *Proceedings of the Nato Advanced Study Institute on Amorphous and Liquid Materials* (Nijhoff, Dordrecht, 1986).
[3]E. Leutheusser, Phys. Rev. A **29**, 2765 (1984).
[4]U. Bengtzelius, W. Götze, and A. Sjölander, J. Phys. C **17**, 5915 (1984), referred to as I.
[5]W. Götze, Z. Phys. B **56**, 139 (1984).
[6]U. Bengtzelius and L. Sjögren, J. Chem. Phys. **84**, 1744 (1986).
[7]D. Forster, *Hydrodynamic Fluctuations, Broken Symmetry, and Correlation Functions* (Benjamin, New York, 1975).
[8]S. P. Das, G. F. Mazenko, S. Ramaswamy, and J. J. Toner, Phys. Rev. Lett. **54**, 118 (1985).
[9]S. P. Das and G. F. Mazenko, Phys. Rev. A **34**, 2265 (1986).
[10]E. Siggia, Phys. Rev. A **32**, 3135 (1985).
[11]T. Taborek, R. N. Kleinman, and D. J. Bishop, Phys. Rev. B **34**, 1835 (1986).
[12]W. Götze, Z. Phys. B **60**, 195 (1985).
[13]W. Götze, *Proceedings of the Nato Advanced Study Institute on Amorphous and Liquid Materials* (Nijhoff, Dordrecht, 1986).
[14]J. J. Ullo and S. Yip, Phys. Rev. Lett. **54**, 1509 (1985).
[15]L. Sjögren, Phys. Rev. A **22**, 2866 (1980); **22**, 2883 (1980).
[16]L. Sjögren and A. Sjölander, J. Phys. C **12**, 4369 (1979).
[17]G. Wahnström and L. Sjögren, J. Phys. C **15**, 401 (1982).
[18]J. L. Lebowitz, J. K. Percus, and J. Sykes, Phys. Rev. **188**, 487 (1969).
[19]A. Z. Akcazu, N. Corngold, and J. J. Duderstadt, Phys. Fluids **13**, 2213 (1970).
[20]H. C. Andersen, D. Chandler, and J. D. Weeks, J. Chem. Phys. **56**, 3812 (1972).
[21]U. Bengtzelius, Phys. Rev. A **33**, 3433 (1986).
[22]S. H. Chen and J. S. Huang, Phys. Rev. Lett. **55**, 1888 (1985).
[23]For a review see K. L. Ngai, Comments Solid State Phys. **9**, 127 (1979); **9**, 141 (1980).
[24]N. O. Birge and S. R. Nagel, Phys. Rev. Lett. **54**, 2674 (1985).
[25]H. De Raedt and W. Götze, J. Phys. C **19**, 2607 (1986).
[26]A. K. Doolittle, J. Appl. Phys. **22**, 1471 (1951).
[27]J. P. Boon and S. Yip, *Molecular Hydrodynamics* (McGraw-Hill, New York, 1980).
[28]R. G. Palmer, D. L. Stein, E. Abrahams, and P. W. Anderson, Phys. Rev. Lett. **53**, 958 (1984).
[29]See, e.g., G. P. Johari, Ann. N.Y. Acad. Sci. **279**, 117 (1976).